Available online at www.sciencedirect.com
ScienceDirect
Journal of Photochemistry and Photobiology A: Chemistry 188 (2007) 25–33
Journal of Photochemistry and Photobiology A:Chemistry
www.elsevier.com/locate/jphotochem

Spectroscopy, photophysical and photochemical properties of bisimidazole derivatives

Natalya Fridman, Menahem Kaftory, Yoav Eichen, Shammai Speiser*

Schulich Faculty of Chemistry, Technion-Israel Institute of Technology, Haifa 32000, Israel

Received 20 August 2006; received in revised form 9 November 2006; accepted 14 November 2006
Available online 19 November 2006

Abstract

Novel bisimidazole derivatives were synthesized and their physico-chemical properties were determined. Different bisimidazole derivatives exhibit solvatochromism, halochromism and photochromism in solution.

We have conducted an investigation of the spectroscopy, photophysical and photochemical properties of all derivatives. The photochemical properties of **1**, **3** and their derivatives, were studied by irradiating acetonitrile solutions with medium-pressure xenon lamp and their photochemical quantum yields, ranging from 0.0011 to 0.0024, together with the corresponding fluorescence quantum yields, ranging from 0.52 to 0.90, and lifetimes, ranging from 1.03 to 1.42 ns, were determined. The photophysics of these bisimidazole derivatives was studied in details. The photochemistry of the two prototype derivatives was studied in solutions, showing an interesting general photochemical reaction between these derivatives and molecular oxygen.

Keywords: Bisimidazole; Lophine; Fluorescence

1. Introduction

Recently, heterocyclic imidazole derivatives have attracted considerable attention because of their unique optical properties [1–3]. These compounds play a very important role in chemistry as mediators for synthetic reactions, primarily as a means for preparing functionalized materials [4–8]. Imidazole nucleus forms the main structure of some well-known components of human organisms, i.e. the amino acid histidine, vitamin B_{12}, a component of DNA base structure, purines, histamine and biotin. It is also present in structure of many natural or synthetic drug molecules, i.e. azomycin, cimetidine and metronidazole [9]. Phenylimidazoles have been studied because of their important laser properties [10,11]. By contrast further substitution by phenyl groups results in other significant optical properties. An important imidazole derivative is lophine (2,4,5-triphenylimidazole). Lophine and its derivatives have significant analytical applications utilizing their fluorescence and chemiluminescence properties [12,13]. Euelgro and co-workers [14] reviewed more applications of other imidazoles.

Some basic processes, such as excited state proton transfer (ESIPT) have been carried out for imidazole derivatives. Molecules that give rise to fluorescent tautomers through ESIPT are useful in lasing systems as laser dyes [10,11], in high-energy radiation detectors [15], molecular energy storage systems [16], and as fluorescent probes [17].

We have studied 2-(2′-hydroxyphenyl)-3*H*-imidazo(4,5-*b*)pyridine, 2-HPIP, and its methylated derivatives which belong to a different class of molecules containing more than one set of proton donor–acceptor couples that may be coupled to one another. Consequently, 2-HPIP is found to form both π- and H-bound dimers in solutions and in the solid state. Their excited-state phototautomerization proton transfer processes in their different aggregation states were determined by studying their absorption and fluorescence spectra at different solvents at a wide range of concentrations [18]. Gostev et al. [19] have studied ESIPT in some lophine (2,4,5-triphenylimidazole, compound **7**, Scheme 1) derivatives, utilizing steady state and femtosecond laser spectroscopy. Bu and co-workers [20] have shown how the fluorescence properties of lophine can be tuned utilizing thiophene and thiazole derivatives. This group had also investigated

* Corresponding author. Tel.: +972 4 8293753; fax: +972 4 8295703.
E-mail address: speiser@techunix.technion.ac.il (S. Speiser).

1010-6030/$ – see front matter © 2006 Elsevier B.V. All rights reserved.
doi:10.1016/j.jphotochem.2006.11.014

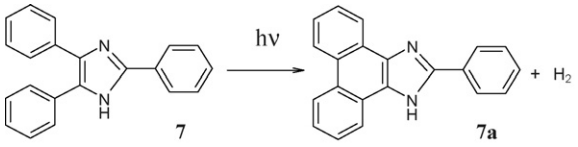

Scheme 1.

some nonlinear optical properties of these and similar compounds. They have stressed the importance of chemical stability of imidazole derivatives for allowing their use in applications such as sensors. The photochemistry of lophine was investigated in solutions by Testa and co-workers [21]. They have found that the photochemistry of **1** is similar to that of stilbene [22] and can be described by the following mechanism (see Scheme 1). They found that the photochemistry of lophine (**7**) leads to 2-phenyl-9,10-phenanthroimidazole (**7a**) and the quantum yield for the photochemical cyclization reaction in degassed acetonitrile solution was $(0.57 \pm 0.07) \times 10^{-3}$. In basic solutions the photochemical reaction is much faster and gives a number of unidentified products at a higher quantum yield.

The presence of an active N–H proton is believed to be the source of photochemical instability. Bu and co-workers [20] attempted to reduce it by specific chemical substitution. They have found evidence that steric effects due to aromatic substitution at the 2-postion in 2,4,5-trisustituted imidazoles have direct impact on the fluorescence properties, which is eliminated by using thiazole at the 2-position. They did not, however, provide any information on the photochemical stability of these compounds.

Recently, we have studied the crystal structure and thermochromic properties of bisimidazole derivatives that form inclusion compounds with hydrogen donating or accepting guest molecules [23]. Our purpose in the present work is to combine these solid-state studies of bisimidazole derivatives with solution spectroscopy investigations that address the same type of interactions. Since applicability of these compounds as optical materials depends on their photochemical stability we have also investigated this aspect.

In the present paper we describe a comprehensive study of the spectroscopy, photophysics and photochemistry of 2,2′-(2,5-thiophenediyl)bis[4,5-diphenyl-1*H*-imidazole] (**1**), 2,2′-(2,5-thiophene-diyl)bis[1-methyl-4,5-diphenyl-1*H*-imidazole] (**2**), 2,2′-(1,4-phenylene)bis[4,5-diphenyl-1*H*-imidazole] (**3**), 2,2′-(1, 4-phenylene)bis[4, 5-bis(4-methoxyphenyl)-1*H*-imidazole] (**4**), 2,2′-(2,5-thiophene-diyl)bis[4,5-bis(4-methoxyphenyl)-1*H*-imidazole] (**5**) and 2,2′-(1,4-phenylene)-bis[1-methyl-4,5-diphenyl-1*H*-imidazole] (**6**). Compounds **2**, **5** and **6** are novel bisimidazoles synthesized for this study.

2. Experimental

All starting materials and solvents were obtained from commercial suppliers and were used as obtained. All synthesized imidazole derivatives were characterized by ^{1}H NMR, mass spectrometry (MS), single crystal X-ray crystallography and by their melting points (m.p.). ^{1}H NMR spectra were recorded on a Bruker AC-400 or AC-500 spectrometer at 298 K. Mass spectroscopy was performed for the analysis of the compounds **1** and **3** (before and after irradiation). Low-resolution chemical ionization (CI) mass spectrometric analysis was carried out on a Finnigan TSQ-700 mass spectrometer with *iso*-butane as carrier gas. High-resolution CI or electron impact (EI) mass spectrometry was investigated on a Autospec Premier instrument with *iso*-butane as carrier gas. MH^+ ion (*m*/*z* 521) for **1** and MH^+ ion (*m*/*z* 515) for **3** were formed before irradiation. Absorption spectra were recorded on a Cary 50 UV–vis spectrophotometer.

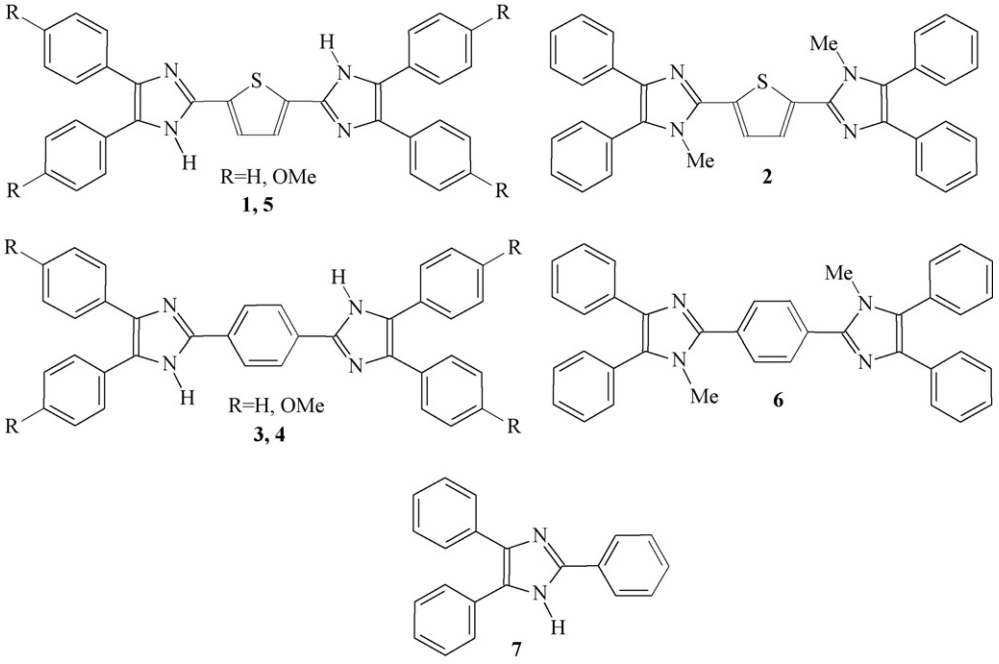

Scheme 2.

Emission and excitation spectra were measured using a Perkin-Elmer LS 50-B spectrofluorimeter. For absorption excitation and emission measurements, the sample concentration was maintained at $\sim 10^{-5}$ M. Spectroscopic grade solvents were used for spectral measurement, without further purification. Excitations at the 320–400 nm region were isolated from an Osram XBO 150 W medium-pressure xenon lamp by using a combination of corning 7–54 and 0–53 filters. Melting points for imidazole derivatives were carried out using a Thermal Analysis DSC Q10.

We prepared a number of bisimidazole derivatives (compounds **1**–**6**, see Scheme 2) utilizing the slightly modified procedure of Davidson et al. [24]. Benzil or 4,4′-dimethoxybenzil (1 mmol), suitable benzaldehyde (0.5 mmol), and ammonium acetate (1.6 g) were dissolved in boiling glacial acetic acid (16 ml) and refluxed for 3–5 h monitored by TLC. The reaction mixture was poured into ice-water and collected on a filter, washed by cold water, dried and recrystallized from the suitable solvent.

2,2′-(2,5-Thiophenediyl)bis[1-methyl-4,5-diphenyl-1*H*-imidazole] **2** and 2,2′-(1,4-phenylene)bis[1-methyl-4,5-diphenyl-1*H*-imidazole] **6** were synthesized, in 70% yield by *N*-methylation of **1** or **3**, respectively, according to the Tanino et al. method [25]. To a solution of **1** or **3** (0.2 mmol, 0.1 g) and dimethyl sulphate (0.72 mmol, 0.066 ml) in 10 ml of acetone was added powdered anhydrous potassium carbonate (0.72 mmol, 0.1 g) and the mixture was refluxed for 4.5 h. After cooling, the mixture was poured into water and the yellow crude was collected by filtration and dried in dessicator. Crystallization of **2** from a 1:1 mixture of MeCN and $CHCl_3$ yields yellow plates **2** (m.p. 295 °C, ^{1}H NMR ($CDCl_3$): δ 7.54 (2H, d), 7.53–7.36 (16H, m), 7.16 (8H, t), 3.66 (6H, s)). Crystallization of **6** from a 1:1 mixture of MeOH and $CHCl_3$ yields colorless needles **6** with the host–guest ratio of (1:2 MeOH) (m.p. 312 °C, ^{1}H NMR ($CDCl_3$): δ 7.54 (4H, d), 7.48 (4H, d), 7.42 (4H, d), 7.22 (8H, t), 7.14 (4H, t), 3.54 (6H, s)).

The dependence of the absorption spectra of each of bisimidazole derivatives in MeCN on the apparent pH was measured by a pH meter with glass electrode. It was changed by adding various amounts of diluted solutions of HCl or NaOH to MeCN.

Fluorescence life-times were determined by using time-correlated single photon counting (TCSPC) methods. We have used the TCSPC experimental set-up in the laboratory of Professor Dan Huppert at Tel-Aviv University, as previously described [26]. Fluorescence quantum yields, Φ_f values were measured with estimated 3% accuracy by using dilute solutions (OD < 0.05) of quinine bisulfate to calibrate the lophine **7** standard which was used as a reference for the determination of fluorescence quantum yields. We obtained the value Φ_f of 0.48 in hexane, as previously reported [20]. Due to the large Stokes shift we could use solutions with OD up to 0.23 without any noticeable inner filter effect giving the same Φ_f values for these OD values as those obtained for OD < 0.1.

(*E*)-α-(2,5-Dimethyl-3-furyl-ethylidene) (isopropylidene) succinic anhydride, or more briefly 3-fulgide, actinometer [27] was used to measure quantum yield of the photochemical reactions. We have checked our method, described below in Section 3.3.1, by measuring the quantum yield for degassed MeCN solution of **7**, reproducing, within our 10% experimental accuracy, the reported literature value of $(0.57 \pm 0.07) \times 10^{-3}$ [21].

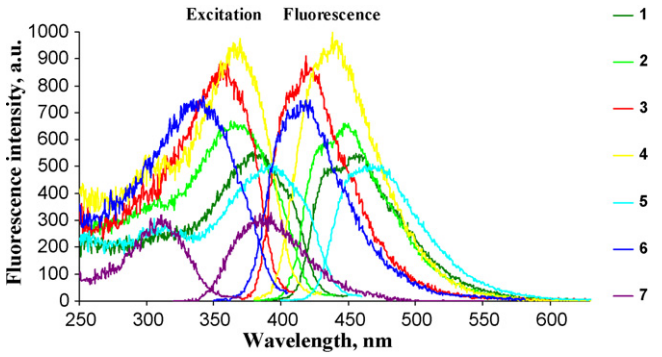

Fig. 1. Excitation (left) and fluorescence spectra (right) of **1**–**7** in MeCN solution.

3. Results and discussion

3.1. Summary of studies in the solid state

Bisimidazole derivatives: 2,2′-(2,5-thiophenediyl)bis[4,5-diphenyl-1*H*-imidazole] **1** and 2,2′-(1,4-phenylene)bis[4,5-diphenyl-1*H*-imidazole] **3** show piezochromism, photochromism and thermochromism in the solid state and form inclusion compounds in various colors. Four solvated compounds in two different colors: yellow and green, depending on the solvent molecules were found for **1** and two different colors: light yellow and colorless were obtained for **3**. Crystal structures of various substituted bisimidazole derivatives are presented elsewhere [23].

3.2. Spectroscopy of (*1*–*7*) in solution

3.2.1. Fluorescence properties

Absorption spectra of bisimidazole derivatives **1**–**6** and lophine **7** were previously reported by us [23]. In addition we have measured the corresponding fluorescence and excitation spectra of those compounds (Fig. 1). Absorption and fluorescence properties of bisimidazole derivatives **1**–**6**, together with the reference spectrum of lophine **7** in MeCN, and lophine **7** where the OD was kept at 0.192 for all solutions, are presented in Table 1. Shown are absorption band maxima λ_{max}, the excitation

Table 1
Absorption and fluorescence data of (**1**–**7**) in MeCN solution

Compound	λ_{max} (nm)	$\lambda(ex)_{max}$ (nm)	$\lambda(fl)_{max}$ (nm)	ΔE (cm^{-1})	Φ_f
1	385	385	458	4140	0.55
2	365	367	452	5124	0.62
3	358	360	424	4193	0.75
4	365	366	440	4595	0.90
5	391	392	470	4234	0.52
6	334	337	417	5693	0.66
7	312	312	387	6229	0.27

spectra band maxima $\lambda(\mathrm{ex})_{max}$, the band fluorescence maxima $\lambda(\mathrm{fl})_{max}$, the peak molar absorptivity ε and the associated Stokes shifts ΔE, together with the fluorescence quantum yields Φ_f.

The values of Φ_f for lophine and all bisimidazole derivatives were calculated using Eq. (1):

$$\Phi_f = \left(\frac{I_{MeCN}}{I_{hexane}}\right)\left(\frac{A_{MeCN}}{A}\right) I \left(\frac{n_{MeCN}}{n_{hexane}}\right)^2 \Phi_{f\ hexane}, \quad (1)$$

where I_{MeCN}, I_{hexane}, I are the integrated fluorescence intensities at the excitation wavelength of lophine **7** in MeCN and *n*-hexane and for (**1**–**6**) in MeCN, respectively. n_{MeCN}, n_{hexane} are the refractive indices of MeCN and *n*-hexane; $\Phi_{f\ hexane}$ the fluorescence quantum yield of the reference lophine **7** sample; A_{MeCN} and A are the absorbance values (at the excitation wavelength) for the reference lophine **7** and for (**1**–**6**) in MeCN. All excitation spectra were recorded while probing the peak fluorescence for each compound, they match the absorption spectra within experimental accuracy.

The fluorescence intensity for benzene bisimidazole derivative increased with adding MeO– substituent in 4,5-phenyl rings (compound **4**) and decreased for thiophene bisimidazole derivative by changing phenyl rings to MeO– substituent in 4,5-phenyl rings (compound **5**). Both **1** and **3** show blue shifted absorption and fluorescence at longer wavelengths as compared to the MeO-substituted compounds **5** and **4**, respectively. Comparison of **1** and **2** indicates that the 1-methyl substituted thiophene bisimidazole derivative **2** shows a blue shifted absorption and fluorescence spectra as compared to the non-substituted thiophene bisimidazole derivative **1**.

3.2.2. *Solvent effect on the absorption and fluorescence properties*

Solvatochromism is the reversible color change induced by solvents. It often results from changes in the polarity of the solvents. This affects charge transfer mechanisms in solvatochromic compounds, causing color changes.

Compound **1** is soluble in many solvents, giving a yellow, lemon or green solution. The positions of the long-wavelength absorption and fluorescence bands in the spectra of **1** were determined in several protic (methanol, acetic acid) and aprotic (acetonitrile, acetone, chloroform, ethyl acetate, ether, THF) solvents. Fig. 2 shows excitation and fluorescence spectra of **1** in various solvents. The solvents used are listed in Table 2, where attempt to correlate the observed absorption and fluorescence energies with the $E_T(30)$, a parameter used for describing the polarity of the solvent [28,29] was done.

Table 2
Solvatochromic properties of **1** in various solvents

Solvent	$E_T(30)$	ν_{max}(ex) (cm^{-1})	ν_{max}(fl) (cm^{-1})	ΔE (cm^{-1})
Methanol	55.1	26,178	21,882	4296
Acetic acid	51.7	25,510	19,881	5629
Acetonitrile	46.0	25,974	21,834	4140
Acetone	42.2	25,974	21,834	4140
Chloroform	39.1	25,317	20,619	4698
Ethyl acetate	38.1	25,974	21,882	4092
THF	37.4	25,907	21,882	4025
Ether	34.5	26,042	22,026	4015

No clear correlation is found, other attempts to correlate the observed solvatochromism with other polarity multi-parameters did not yield any better result. This is not surprising since the solvent effects for these bisimidazole derivatives are a complex mixture of polarity effects as well as more specific interactions such as hydrogen bonding and the acidity correlated with the –NH proton. Unfortunately these compounds do not dissolve in nonpolar solvent such as hexane or cyclohexane, which usually can provide the reference point for the discussion of solvatochromism. The excitation and emission spectra in all solvents except chloroform and acetic acid are practically the same independent of the polarity. This may indicate that specific interactions play the major role in these solvents [28,29]. The common feature of these solvents is the presence of a lone pair of electrons, which can form an H-bond with the N–H group of compound **1**. This assumption is supported by our previous observations in nitro derivatives of lophine where the N–H group is replaced by N–Me [30]. In acetic acid, the red shift of the emission may be the result of the excited state protonation.

3.2.3. *Halochromism in MeCN solution*

Halochromism is the reversible color change due to a change in pH of a solution. Compound **1** showed halochromic behavior with changing the apparent pH in MeCN solution. The excitation

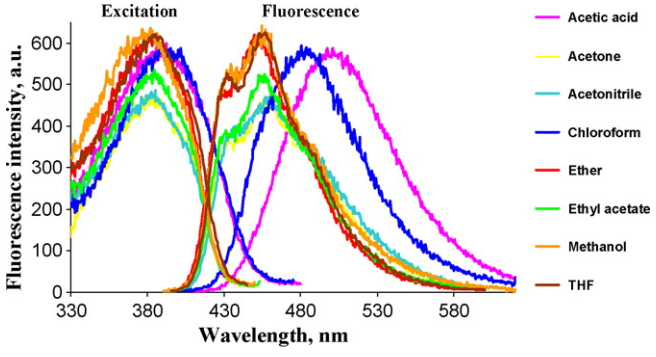

Fig. 2. Excitation (left) and fluorescence spectra (right) of **1** in various solvents: violet, acetic acid; yellow, acetone; light blue, acetonitrile; blue, chloroform; red, ether; green, ethyl acetate; orange, methanol; brown, THF.

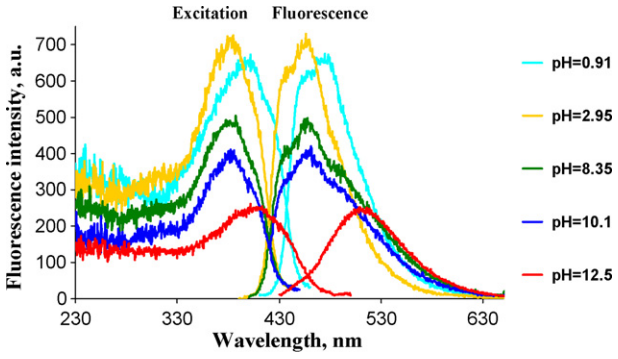

Fig. 3. Excitation and fluorescence spectra of **1** at different apparent pH meter readings, in $C \sim 10^{-5}$ M MeCN solution.

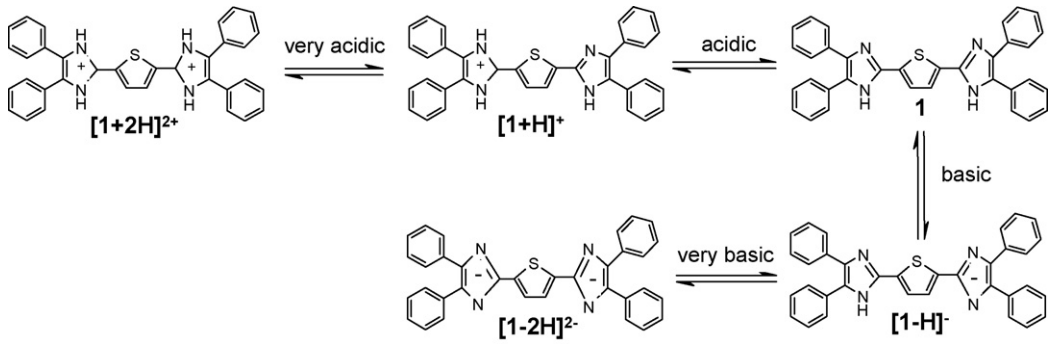

Scheme 3.

and fluorescence spectra of **1** at different pH in MeCN solution are presented in Fig. 3. It was shown that λ_{max} increases with increasing pH, while the fluorescence intensity decreases with increasing pH. In case of a very acidic MeCN solution (apparent pH 0.91) the absorbance band observed at $\lambda_{max}(ex) = 373$ nm, whereas in case of very basic MeCN (apparent pH 12.5) solution the absorbance band is red shifted to $\lambda_{max}(ex) = 388$ nm. The fluorescence intensity gradually reduces with increasing pH. In very basic MeCN solution the product almost does not exhibit any fluorescence. The fluorescence band maximum (Fig. 3) is observed at $\lambda_{max}(fl) = 478$ nm at very acidic solution, whereas at $\lambda_{max}(fl) = 516$ nm at very basic solution. In the absorption spectra [23] two clear isosbestic points observed at 329 and 382 nm and two unclear isosbestic points observed at 282 and 344 nm depending on pH suggest the presence of four different possible species of **1** (see Scheme 3). Fig. 4 represents the energies of absorption (ν_a) and fluorescence (ν_f) transitions of **1** in MeCN as a function of pH. Calculated p*K*a values are: $pKa_1 = 11.39 \pm 0.5$, $pKa_2 = 3.69 \pm 0.16$ [31].

3.3. Photochemistry of *1–7* in MeCN solution

3.3.1. Determination of the photochemical quantum yields

All bisimidazole derivatives undergo photochemical reactions. We have compared the photochemical properties of all bisimidazole derivatives with that of lophine **7** [21]. We describe in details the photochemistry of **1** in MeCN, the same procedure was applied to all bisimidazole derivatives, yielding similar results.

The photochemical properties of **1** were studied by irradiating 1×10^{-5} M basic and neutral degassed MeCN solutions of compounds **1**. Both MeCN solutions of **1** were irradiated with medium-pressure xenon lamp (150 W). The absorption spectra of **1** in neutral MeCN solution for different irradiation times are presented in Fig. 5. A clear isosbestic points at 420 nm is observed. This is indicative of a single photochemical product. By contrast, for basic MeCN solution no clear isosbestic points are observed. This suggests that there may be more than two species formed in the system at each basic solution, in agreement with previous studies done on lophine **7** [21]. Fig. 5 shows a comparison between the absorption spectrum of **1** and that of the product obtained after 100 min irradiation, showing the total disappearance of the 380 nm band with the appearance of a weak absorption in the 425–550 nm spectral region, which can be attributed to the photochemical product of the cyclization reaction similar to that of **7**, described in Scheme 1 and found in the high-resolution MS analysis of the reaction products.

Comparison of the fluorescence maxima in three solutions with different pH values revealed that the fluorescence intensity of **1** in neutral degassed MeCN solution is higher than that of **1** in basic MeCN solution. The rate of the reaction in basic MeCN solution of **1** was almost eight times larger than in the non-degassed MeCN solution. These observations are similar to

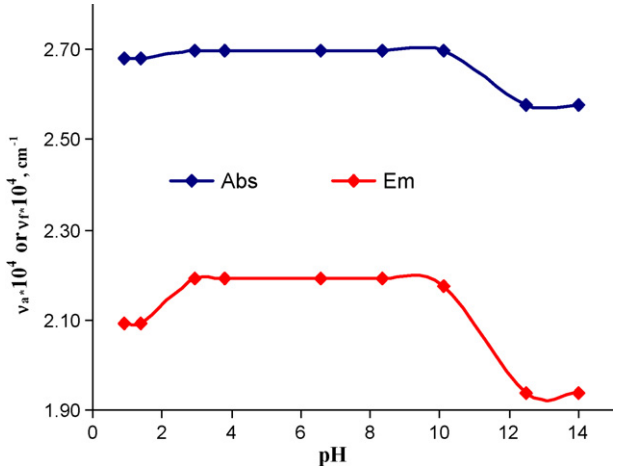

Fig. 4. Transition energies of absorption (ν_a) and fluorescence (ν_f) vs. apparent pH meter readings for **1** in $C \sim 10^{-5}$ M MeCN solution.

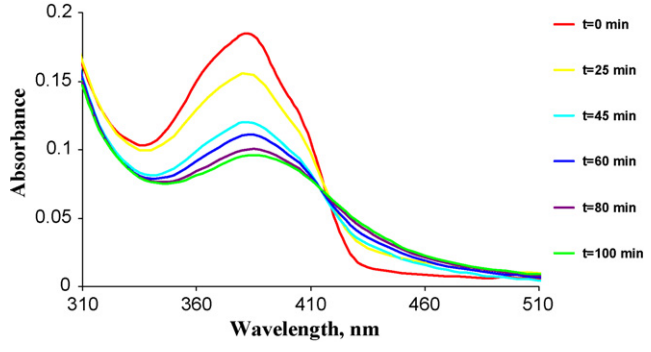

Fig. 5. Absorption spectra of **1** in neutral degassed $C \sim 10^{-5}$ M MeCN solution with different irradiation time duration: 0, 25, 45, 60, 80, and 100 min (from top to bottom).

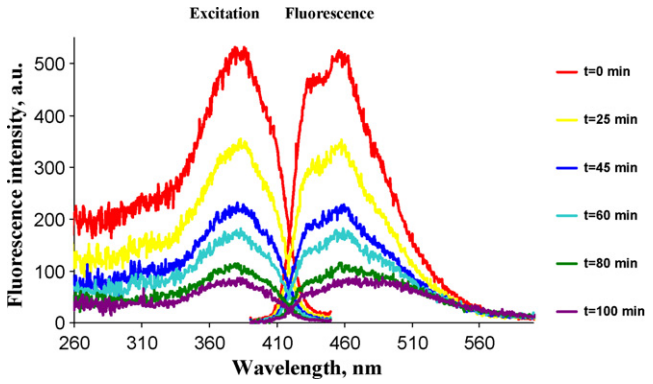

Fig. 6. Excitation and fluorescence spectra of **1** at different irradiation times in neutral degassed $C \sim 10^{-5}$ M MeCN solution.

those reported for lophine **7** under similar conditions [21], for which in degassed solution the yield is about five times smaller than in non-degassed solution.

The excitation and fluorescence spectra of **1** at different irradiation times in degassed MeCN solution are shown in Fig. 6. The photochemical product is almost non-fluorescent. The fluorescence intensity gradually reduces with irradiation time. The fluorescence spectra and their kinetics features remain unchanged for all excitation wavelengths in the region of 245–400 nm. The rate of the photochemical reaction for the given irradiation intensity is shown to obey a first order law kinetics and can be quantified either from the absorption data or from the excitation and fluorescence data in Fig. 7. It is satisfying to note that the same rate constant, k_r is obtained from all these different data. However, the kinetics of the fluorescence changes in the 500–560 nm range are non-exponential since at this region we have contributions both from the disappearance of the starting material **1** as well as build up of the weak product fluorescence, which is red shifted to that of **1**.

For an optically thin sample, the experimental photochemical rate constant for the disappearance of **1** is given by $k_r = \Phi_r \sigma I$, where Φ_r is the reaction quantum yield, σ the absorption cross-section and I is the irradiation light intensity. In order to determine the Φ_r values for compounds (**1**–**7**) we have used the photoisomerization of (*E*)-α-(2,5-dimethyl-3-furyl-ethylidene) (isopropylidene) succinic anhydride (3-fulgide), as a photochemical actinometer [27] for the determination of the quantum yields of the photolysis reactions of (**1**–**7**).

The Φ_r^1 values for lophine **7** and bisimidazole derivatives (**1**–**6**) are calculated based on Eq. (2):

$$\Phi_r^1 = \frac{k_r^1 \sigma_r \Phi_r}{\sigma_r^1 k_r} = \frac{k_r^1 \varepsilon_r \Phi_r}{\varepsilon_r^1 k_r}, \quad (2)$$

where k_r^1, are the rate constants for the phothochemical reaction of compounds (**1**–**7**), k_r the corresponding measured value for 3-fulgide under the same irradiation conditions, ε_r^1 and ε_r are the molar extinction coefficients for in MeCN and for 3-fulgide in EtOH [27], respectively. Φ_r is the quantum yield of the photoisomerization of 3-fulgide which is 0.22 in EtOH [27b]. The photochemical quantum yields for (**1**–**7**) are summarized in Table 3, together with the corresponding fluorescence quantum yields. Although the photochemical quantum yields are rather large so as to render these compound photochemically unstable for any optical application, they do not influence the measurements of the fluorescence quantum yields which were

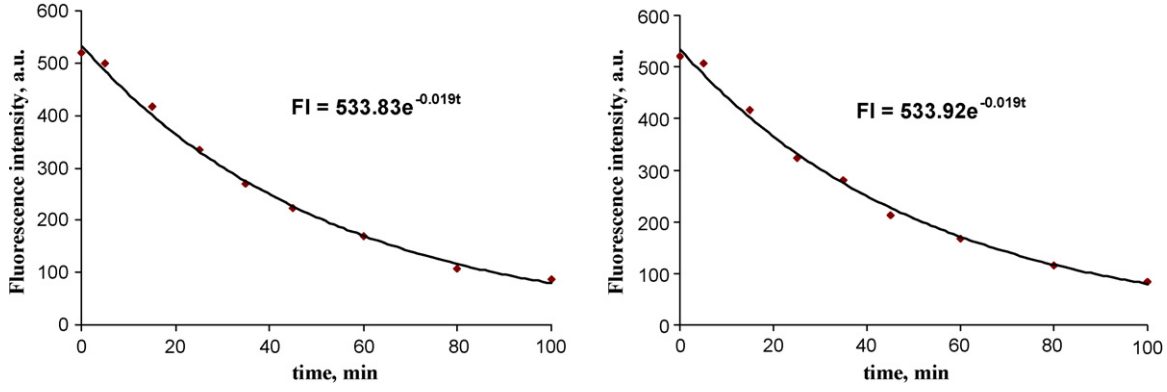

Fig. 7. Photochemical reaction kinetics: excitation spectrum intensity (left) at 384 nm, probed at 456 nm and fluorescence spectrum intensity (right) at 456 nm, probed at 384 nm of **1**, as a function of the irradiation time, in neutral degassed MeCN solution.

Table 3
Comparison of the fluorescence and photochemical characteristics of (**1**–**7**), in degassed MeCN solution

Compound	$\lambda(ex)_{max}$ (nm)	ε (M^{-1} cm^{-1})	k_r ($\times 10^{-4}$ s^{-1})	Φ_f	Φ_r	τ_f (ns)	k_{rad} (ns^{-1})	k_{nr} (ns^{-1})
1	385	34,870	3.17	0.55	0.0024	1.03	0.53	0.43
2	367	20,350	1.83	0.62	0.0024	1.42	0.44	0.27
3	360	14,860	0.67	0.75	0.0012	1.11	0.68	0.23
4	366	43,910	1.83	0.90	0.0011	1.24	0.73	0.08
5	392	47,820	5.01	0.52	0.0027	1.24	0.42	0.39
6	337	15,470	0.72	0.66	0.0012	1.10	0.60	0.31
7	312	20,330	0.40	0.27	0.0005	1.98	0.14	0.38

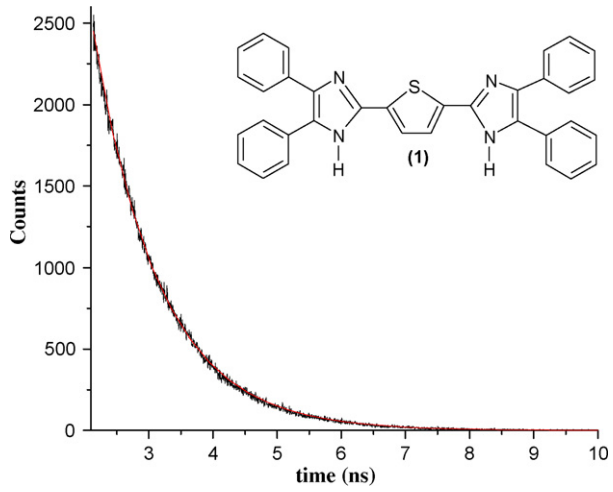

Fig. 8. Fluorescence decay for **1** in MeCN solution (OD = 0.2).

done by excitation in a fluorimeter whose irradiation intensity is much smaller that that of the photolysis lamp. In fact no photochemical degradation was detected following the fluorescence measurements.

It should be noted that the assumption of an optically thin sample may lead to erroneous results in cases where a significant attenuation of the irradiated beam is observed. By placing a calibrated photodiode before and after the reaction cell we have verified that it did not happen, probably due to the fact that we have used rather intense lamp so that the average number of photons vastly exceeds the number of molecules. This is also reflected by the fact that first order kinetics was observed for irradiation times up to 500 min. Moreover, the linear dependence of k_r on I was verified by changing the irradiation intensity by ND filters. We also measured Φ_r for our reference compound **7**, by irradiating both our sample and the actinometer till the irradiated compound totally disappeared (about 600 min), thus determining the absolute number of absorbed photons, and obtained the same value for Φ_r within the estimated 10% accuracy.

We have also measured the fluorescence decay kinetics of compounds (**1**–**7**). All compounds showed exponential decay with life-times τ_f, ranging between 1.03 and 1.98 ns, as exemplified for **1** in Fig. 8. All τ_f values are summarized in Table 3:

$$\Phi_f = \frac{k_{rad}}{k_{rad} + k_{nr}} = \tau_f k_{rad}, \quad (3)$$

where k_{rad}, k_{nr} are the rate constants for radiative and non-radiative deactivation and τ_f is the lifetime of the S_1 excited state. It is evident that the main decay route of the excited state in these compounds is their fluorescence and non-radiative decay which has minor contribution from the photochemical decay route.

From the measured value of Φ_r of **1** the intrinsic unimolecular rate constant for its photochemical decay, $k'_r = \Phi_r/\tau_f = 2.4 \times 10^6\ s^{-1}$ is calculated, a reasonable value.

3.3.2. *The photochemistry of **1** and **3** in non-degassed MeCN and THF solutions: product analysis and proposed mechanisms*

We have also repeated the same photochemical experiments for**1** and for **3** in non-degassed MeCN and THF. The kinetics did not follow a first order law and no clear isosbestic points were observed, suggesting that more than one photochemical product was produced. The nature of the different photoproducts of these solutions was revealed using high-resolution mass spectroscopy.

Irradiation of **1** in non-degassed MeCN and THF solutions, results with the gradual disappearance of the molecular peak at $m/z = 521.1810$ [$M + H^+ = 521.1813$] and parallel appearance of new peaks at $m/z = 122.0600$, 211.0753, 226.0878 and 328.0908. These m/z values correspond to the species **1A** [benzamide, C_7H_7NO, $M + H^+ = 122.0606$], **1B** [1,2-diphenylethane-1,2-dione (Benzil), $C_{14}H_{10}O_2$, $M + H^+ = 211.0759$], **1C** [4,5-diphenyl-3*H*-[1,2,3]dioxazole, $C_{14}H_{11}NO_2$, $M + H^+ = 226.0868$] and **1D** [5-(4,5-diphenyl-1*H*-imidazole-2-yl)-thiophene-2-carbonitrile, $C_{20}H_{13}N_3S$, $M + H^+ = 328.0908$] in addition we detected fragment A at a $z/e = 537.1815$ [5-(4,5-diphenyl-1*H*-imidazole-2-yl)-*N*-[2-oxo-1,2-diphenyl-eth-(*E*)-ylidene]-thiophene-2-carboxamidine, $C_{34}H_{25}N_4OS$, $M + H^+ = 537.1749$] (see Scheme 4).

While **1A** and **1B** are clearly products of a multistep fragmentation **1A** and simple non-photochemical hydrolysis (due to traces of water present always in commercial analytical or spectroscopic grade solvents) **1B**, compounds **1C** and **1D** provide some insight to the photochemical decomposition channels of **1**. From the nature of the dominant fragments, a mechanism may be deduced, involving photoinduced molecular oxygen attack on the imidazole ring. Fig. 9 depicts the proposed mechanism of the major photochemical processes, as deduced from the nature of the major photoproducts that were identified in the mass spectra. The occurrence of fragment **1E** of the intermediate **Int** is an additional support for the proposed mechanism.

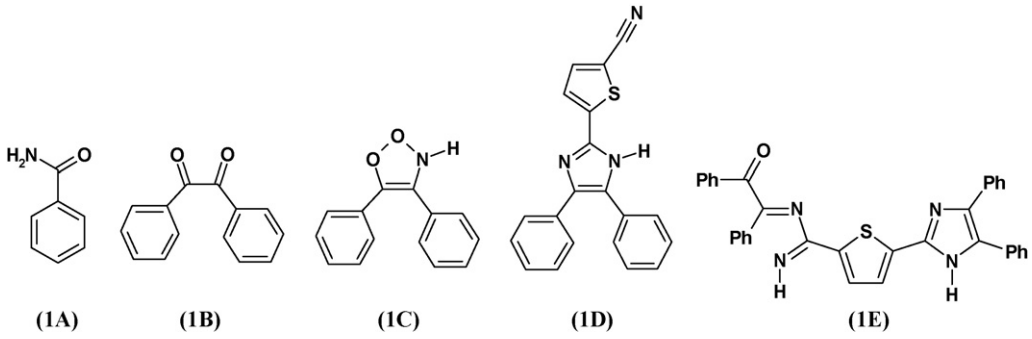

Scheme 4.

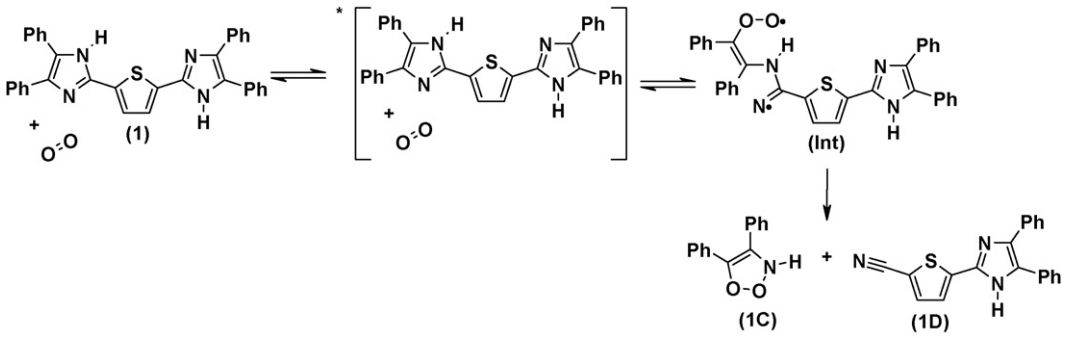

Fig. 9. Proposed mechanism for the photochemical decomposition of **1** in MeCN and THF.

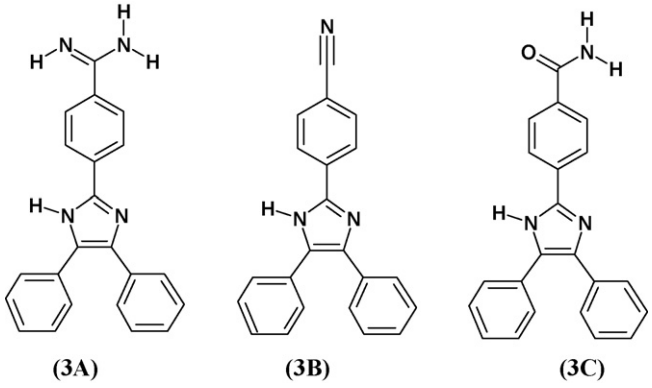

Scheme 5.

Irradiation of **3** in MeCN results with the gradual disappearance of the molecular peak at $m/z = 515.2213$ [$M + H^+ = 515.2236$] and parallel appearance of one dominant new peak at $m/z = 339.1612$. This m/z value corresponds to **3A** [4-(4,5-diphenyl-1*H*-imidazole-2-yl)-benzamidine, $C_{22}H_{18}N_4$, $M + H^+ = 339.1610$] (see Scheme 5). From the nature of the dominant fragment at $m/z = 339.1612$, a mechanism may be deduced, involving a photoinduced hydrolysis of the imidazole ring that involves molecular oxygen. Fig. 10 depicts the proposed mechanism of the major photochemical processes, as deduced from the nature of the major photoproduct that was identified in the mass spectra.

Irradiation of **3** in THF results with the gradual disappearance of the molecular peak at $m/z = 515.2213$ [$M + H^+ = 515.2236$] and parallel appearance of new peaks at $m/z = 122.0608$, 226.0872, 322.1353 and 340.1443. These m/z values correspond to the species **1A**, **1C** (see Scheme 4), **3B** [5-(4,5-diphenyl-1*H*-imidazole-2-yl)-thiophene-2-carbonitrile, $C_{22}H_{15}N_3$, $M + H^+ = 322.1344$] and **3C** [4-(4,5-diphenyl-1*H*-imidazole-2-yl)-benzimidic acid, $C_{22}H_{18}N_3O$, $M + H^+ = 340.1450$] (see Scheme 5).

While **1A** is clearly a product of a multistep fragmentation and the route to compound **1C** is similar to the mechanism depicted in Fig. 9, **1C** and **1B** are formed through a mechanism that is similar to the one depicted in Fig. 9.

For all photolysis reactions depicted in Figs. 9 and 10, none of the mass spectra could reveal any product that involves or originates from a diphenyl ethane to phenanthrene cycloaddition reaction, the dominant reaction that was deduced for lophine **7** (see Scheme 1) [15], based on UV spectroscopy. However, the novel route involving molecular oxygen could not be deduced without employing the sensitive method of high-resolution mass spectrometry. Since we do not observe any molecular peak originating from a phenanthrene derivative, we conclude that this mechanism is not effective in the photochemistry of **1** and **3**, in the presence of oxygen.

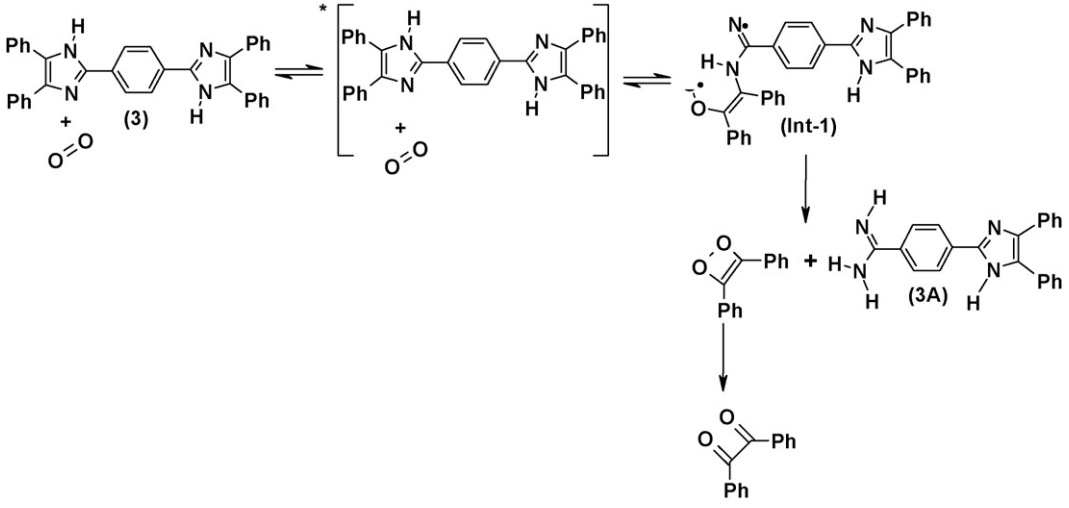

Fig. 10. Proposed mechanism for the photochemical decomposition of **3** in MeCN.

4. Summary

Bisimidazole derivatives were synthesized and their physicochemical properties were determined. The photochemical properties of **1** and **3** and their derivatives were studied by irradiating basic and neutral degassed MeCN solutions with medium-pressure xenon lamp and their photochemical quantum yields, ranging from 0.0011 to 0.0024, together with the corresponding fluorescence quantum yields, ranging from 0.52 to 0.90, and life-times, ranging from 1.03 to 1.42 ns, were determined. It was concluded that the main decay route of the excited state in all these compound is via a combination of fluorescence and non-radiative decay. However, even these values for the photochemical quantum yields make the compounds photochemically unstable. The photochemistry of the two prototype derivatives revealed an interesting novel general photochemical reaction between these derivatives and molecular oxygen.

Acknowledgements

This research was supported by the Fund for the Promotion of Research at the Technion and the Technion VPR Fund.

References

[1] J. Santos, E.A. Mintz, O. Zehnder, C. Bosshard, X.R. Bu, P. Gunter, Tetrahedron Lett. 42 (2001) 805.
[2] X.R. Bu, H. Li, D. Van DerVeer, E. Mintz, Tetrahedron Lett. 37 (1996) 7331.
[3] H. Li, J. Santos, D. Van DerVeer, E.A. Mintz, X.R. Bu, in: T.L. Coleman, B. White, S. Goodman (Eds.), Proceedings of the NASA URC Technical Conference, vol. III, 1998, p. 671.
[4] T. Kamidate, K. Yamaguchi, T. Segawa, H. Watanabe, Anal. Sci. 5 (1989) 429.
[5] (a) K. Nakashima, H. Yamasaki, N. Kuroda, S. Akiyama, Anal. Chim. Acta 303 (1995) 103;
(b) K. Nakashima, Biomed. Chromotogr. 17 (2003) 83.
[6] A. MacDonald, K.W. Chan, T.A. Nieman, Anal. Chem. 51 (1979) 2077.
[7] D.F. Marino, J.D. Ingle Jr., Anal. Chem. 53 (1981) 294.
[8] B.H. Lipshutz, Chem. Rev. 86 (1986) 795.
[9] U. Üçucu, N.G. Karaburun, İ. Işikdağ, IL Farmaco 56 (2001) 285.
[10] (a) P.T. Chou, T.J.A. McMorrow, M. Kasha, J. Phys. Chem. 88 (1984) 4596;
(b) P.T. Chou, M.L. Martinez, Radiat. Phys. Chem. 41 (1993) 373.
[11] A. Parkenopoulos, M. Kasha, Chem. Phys. Lett. 146 (1987) 77.
[12] K. Nakashima, Y. Taguchi, N. Kuroda, S. Akiyama, G. Duan, J. Chromatogr. 619 (1993) 1.
[13] K. Yagi, C.F. Soong, M. Irie, J. Org. Chem. 66 (2001) 5419.
[14] J. Catalan, J.L.M. Abboud, J. Euelgro, Basicity and acidity of azoles Advances in Heterocyclic Chemistry, vol. 41, Academic Press, 1987, pp. 187–274.
[15] L.A. Harrah, C.L. Renschler, Nucl. Instrum. Methods Phys. Rev. A235 (1985) 41.
[16] T. Nishiya, S. Yamuchi, N. Hirota, M. Baba, I.J. Hamazaki, Phys. Chem. 90 (1986) 5730.
[17] A. Sytnik, J. Carlos Del Valle, J. Phys. Chem. 99 (1995) 13028.
[18] H. Salman, S. Meltzman, S. Speiser, Y. Eichen, J. Lumin. 102–103 (2003) 261.
[19] F.E. Gostev, L.S. Kol'tsova, A.N. Petrukhin, A.A. Titov, A.I. Shiyonok, N.L. Zaichenko, V.S. Marevtsev, O.M. Sarkisov, J. Photochem. Photobiol. A 156 (2003) 15.
[20] K. Feng, F.-L. Hsu, Van DerVeer, K. Bota, X.R. Bu, J. Photochem. Photobiol. A 165 (2004) 223.
[21] J. Hennessy, A.C. Testa, J. Phys. Chem. 76 (1972) 3362.
[22] (a) C.S. Wood, F.B. Mallory, J. Org. Chem. 29 (11) (1964) 3373;
(b) F.B. Mallory, C.S. Wood, J.T. Gordon, J. Am. Chem. Soc. 86 (1964) 3094.
[23] N. Fridman, S. Speiser, M. Kaftory, Cryst. Growth Des. 6 (7) (2006) 1653.
[24] D. Davidson, M. Weiss, M. Jelling, J. Org. Chem. 2 (1937) 319.
[25] H. Tanino, T. Kondo, K. Okada, T. Goto, Bull. Chem. Soc. Jpn. 45 (1972) 1474.
[26] P. Leiderman, L. Genosar, D. Huppert, J. Phys. Chem. 109 (2005) 5965.
[27] (a) P.J. Darcy, H.G. Heller, P.J.J. Strydom, Chem. Soc., Perkin. Trans. 1 (1981) 202;
(b) H.G. Heller, J.R. Langan, Chem. Soc., Perkin. Trans. 1 (1981) 341.
[28] C. Reinhardt, Chem. Rev. 94 (1994) 2319, and references therein.
[29] B. Valeur, Molecular Fluorescence, Wiley-VCH, 2002 (Chapter 7, and references therein).
[30] N. Fridman, S. Speiser, M. Kaftory, Cryst. Growth Des. 6 (10) (2006) 2281.
[31] Calculated Using, Advanced Chemistry Development (ACD/Labs) Software V8.14 for Solaris (©1994–2006 ACD/Labs).